ELSEVIER

Journal of Alloys and Compounds 434–435 (2007) 707–709

Journal of ALLOYS AND COMPOUNDS

www.elsevier.com/locate/jallcom

Microstructures and phase formations in the surface layer of an AISI D2 steel treated with pulsed electron beam

J.X. Zou [a,b,1], T. Grosdidier [b,*], K.M. Zhang [a,2], B. Gao [a,3], S.Z. Hao [a,3], C. Dong [a,4]

[a] *State Key Laboratory of Materials Modification & School of Materials Science and Engineering, Dalian University of Technology, Dalian 116024, PR China*

[b] *Laboratoire d'Etude des Textures et Applications aux Matériaux (LETAM, UMR-CNRS 7078), Université Paul Verlaine Metz, Ile du Saulcy, 57045 Metz, France*

Available online 17 October 2006

Abstract

The nanostructures and metastable phase transformations in the surface layer of an AISI D2 steel treated with high current pulsed electron beam (HCPEB) were investigated. The surface structure is marked by two distinct features, i.e. the formation of sub-micrometer fine austenite γ grains (50–150 nm), and the disappearance of carbides via dissolution and crater eruption. The γ phase directly grows from the melt and is retained down to room temperature. Although the cooling rate is as high as 10^7 K/s in our case, the martensitic transformation could completely be suppressed. Such an effect is due to the increased stability of the austenite phase through grain refinement and chemistry modification.

Keywords: Nanostructured materials; Thin films; Rapid solidification; Electron beam processing; Phase transitions

1. Introduction

Recently, the application of energetic beams such as ion, electron, laser and plasma has been of increasing interest to modify the surface of metallic materials [1–5]. Among these techniques, the high current pulsed electron beam (HCPEB) is relatively new [4,5]. The simplicity and reliability of this technique renders special advantages over laser and ion beam treatments, with potential industrial applications [4].

After the HCPEB treatment, the surface properties are determined by the final structure-phase states. However, limited amount of work has concentrated on detailed microstructure characterization of HCPEB treated surface. Previous studies have, for example, shown that the HCPEB treatment leads to a significant improvement in the wear and fretting resistances of die steels [5], but detailed investigations of the structure and phase evolutions in HCPEB treated steels are still missing. The purpose of this work is therefore to study the microstructures and phase transformations in the melted surface layer of the AISI D2 steel after the HCPEB treatment.

2. Experimental equipment and sample preparation

The electron beam system used in this work is a "Nadezhda-2" type HCPEB source [4,5]. It can produce electron beams with the following characteristics: an electron energy of 10–40 keV; a pulse duration of about 1 μs; an energy density ranging from 0.5 to 5 J/cm^2 and a cross-section area that can be adjusted between 10 and 50 cm^2.

A typical cold worked die steel AISI D2 was studied in this work. Its chemical composition and transformation temperatures are shown in Table 1. Before the electron beam treatment, samples were machined to dimensions of 25 mm × 10 mm × 10 mm and austenitized at 1020 °C for 30 min. Water quenching terminated this heat treatment. The steel was subsequently tempered at 200 °C for 3 h. The sample surface was prepared before the HCPEB treatment by mechanical polishing to ensure a similar initial surface state (Ra about 0.07 μm). The energy of the electron beam was kept constant at 27 keV and different pulse numbers were used (5 and 25 times). For all treatments, the pulsing time was about 1 μs and 10 s were set between each pulse.

3. Results

Fig. 1 shows the typical surface morphology of a sample that was HCPEB treated for 5 pulses. The typical feature on the surface is the formation of craters, which is a common feature of

* Corresponding author. Tel.: +33 387317130; fax: +33 387315377.
E-mail addresses: jianxin.zou@univ-metz.fr (J.X. Zou), thierry.grosdidier@univ-metz.fr (T. Grosdidier), zhangkm@student.dlut.edu.cn (K.M. Zhang), surf_gao@yahoo.com.cn (B. Gao), shengzhi_hao@yahoo.com.cn (S.Z. Hao), dong@dlut.edu.cn (C. Dong).
[1] Tel.: +33 387317130; fax: +33 387315377.
[2] Tel.: +86 411 84708441.
[3] Tel.: +86 411 84708380; fax: +86 411 84708389.
[4] Tel.: +86 411 84707930/11; fax: +86 411 84708389.

0925-8388/$ – see front matter © 2006 Elsevier B.V. All rights reserved.
doi:10.1016/j.jallcom.2006.08.280

Table 1
The composition and transfer temperature of AISI D2 steel

Samples	Chemical composition (wt.%)						Transformation temperature (°C)			
	C	Mn	Si	Cr	Mo	V	Ac_1	Ac_m	Ar_1	Ms
D2	1.40–1.60	≤0.60	0.60	11.00–13.00	0.70–1.20	≤1.10	810	982	760	230

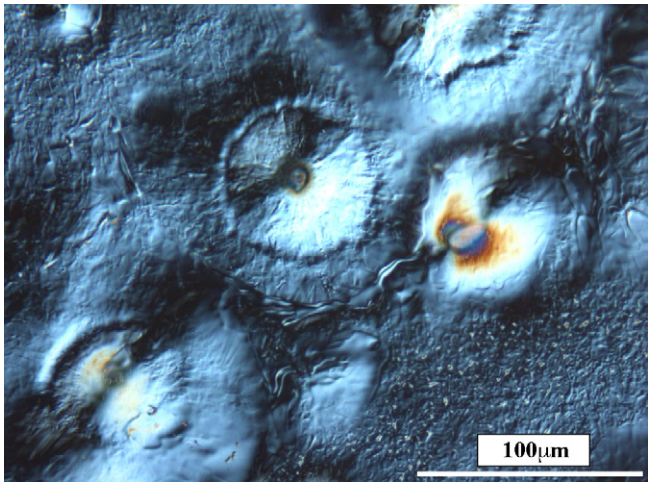

Fig. 1. Typical optical surface morphology of the sample treated with 5 pulses.

many HCPEB treated metal surfaces [4]. The center of the crater often has a special contrast. EDX analysis have shown that Cr carbides are very often located in the center of the craters. The Cr_7C_3 carbides have lower melting point and heat conductivity than the α ferrite matrix, so they serve as nucleation sites for the eruption events that lead to the formation of craters. On the other hand, a part of the carbides, which are not involved in the crater formation, will be dissolved during melting.

Fig. 2 shows a typical cross-sectional micrograph of the treated sample after 25 pulses. The "white" continuous layer visible on the surface corresponds to the melted layer that is known to be weakly echable [4]. The average depth of the melted layer is 4.4 μm after 25 pulses.

XRD analysis was carried out on the samples before and after the HCPEB treatments to study the phase transformation in the melted layer. Fig. 3a shows the evolution of the XRD traces with the number of pulses. As mentioned previously, the initial sample mainly contained two phases: ferrit (α-Fe) and carbide Cr_7C_3. After the HCPEB bombardment, the XRD traces changed somehow dramatically. Firstly, the peaks of the Cr_7C_3 carbide disappeared after the HCPEB treatments. This is due to dissolution of this phase, as was suggested by the OM observations of the cross-section. Secondly, in the sample treated for 5

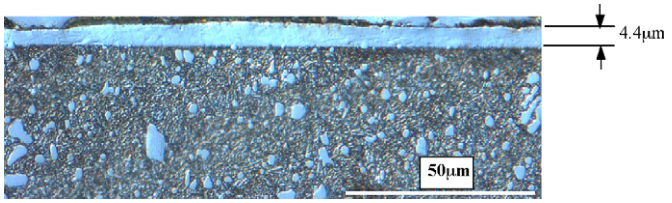

Fig. 2. Cross-sectional optical morphology of the 25 pulsed sample.

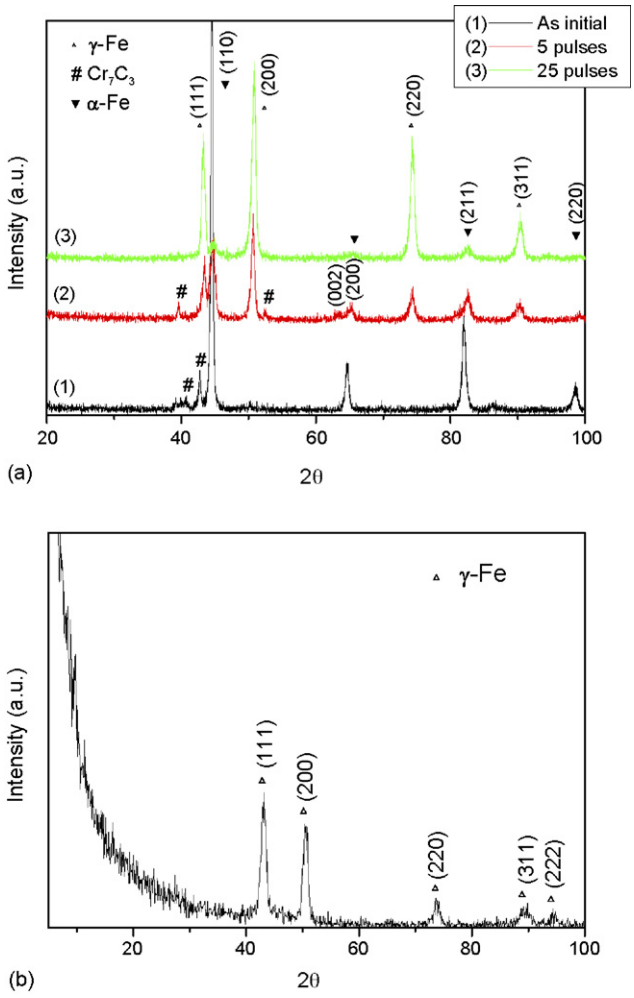

Fig. 3. (a) XRD patterns of the untreated and treated samples. (b) Low incident beam XRD pattern of the 25 pulsed sample.

pulses, a splitting of the (2 0 0) peak is observed. Such kind of peak splitting is usually found in the newly formed martensite. Finally, some new peaks appear in the XRD traces. They were verified to be from the γ-Fe phase. The peak intensity of the γ-Fe phase increases with the number of pulses, indicating that the volume fraction of the γ phase detected by XRD increases.

Fig. 3b shows the low incidence beam X-ray diffractogram recorded on the sample treated for 25 pulses. It only shows the presence of the γ peaks. This indicates that the surface layer is mainly composed of the γ phase. Since γ is a high temperature phase, it should transform after solidication into martensite because of the very high cooling rate (~10^7 K/s) undergone by the surface of the sample due to heat conduction towards the bulk [6,7]. Therefore, the observation of such a high amount of γ phase at the surface is somehow fairly unusual.

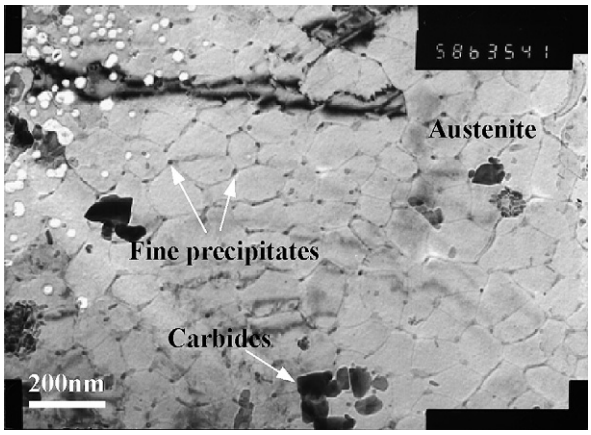

Fig. 4. Typical TEM morphology in the melted layer of the 25 pulsed sample.

Fig. 4 shows a typical TEM bright field image from the melted layer of a 25 pulsed sample. Very fine carbides, having an average size ranging from 20 to 100 nm, are visible in some locations (arrowed). These carbides were often present in groups. Their small size suggests that they are not completely dissolved carbides. The majority of the structure consisted however of the γ phase. The subgrain size of the γ phase was in the range of 50–150 nm. A careful look at the micrograph in Fig. 4 reveals also very fine precipitates. Their size is below 10 nm. They are often present at the subgrain boundaries and in particular most often at triple junctions, as arrowed in Fig. 4. Their presence at subgrain boundary triple junction suggest that they precipitated from the solid state. Finally, it is also interesting to note that no dislocations are present in the austenite subgrains.

4. Discussions

The HCPEB bombardment gives rise to superfast heating and melting, followed by rapid solidification in the melt zone of the material. This makes it possible to produce metastable states in the surface layers of the materials. This is for example the case of the fine grained γ phase which is retained down to room temperature. In addition, it is clear that depending on the energy transferred to the material (i.e. 5 and 25 pulses) the degree of metastability of the melted layer is quite different.

From the phase diagram, it can be established that the primary phase in solidification for the D2 steel should be γ. However, under our metastable conditions, the selection of the primary phase will depend on the local composition of the liquid and its under cooling. Under HCPEB, as the existence time in the melt is very short, the composition may not be completely homogeneous everywhere. This is particularly true for the low number of pulses because the carbides are not dissolved completely. Therefore, the actual composition of the melt is locally different and the primary phase may not be the γ phase. When the pulse number increases, the composition becomes more homogenous. This corresponds to an increase in the γ content in the surface layer. After solidification, during the cooling process, solid state transformation should be operative. Considering that the cooling rate can be as high as 10^7 K/s [6], the diffusion types of transformations, such as the $\gamma \rightarrow \alpha + C$ for instance, are suppressed while only the martensitic transformation ($\gamma \rightarrow \alpha'$) should be possible. However, the interesting phenomenon found in the present work is the stabilization of the austenite, despite the martensitic transformation point (Ms) being 230 °C (Table 1). Indeed no martensite was observed in the surface layer of the samples treated for 25 pulses. From the theory of martensite [8,9], the martensitic transformation is also a nucleation process, and it depends on the state of the austenitic matrix. In our case, the γ phase directly grows from the melt during the rapid solidification process and the dissolution of Cr and C in this phase will significantly enhance its strength. This is an important factor for the stabilization of the γ phase [8,9]. In addition, the very fine subgrain size is another factor for the stabilization of the γ phase because it is harder for it to transform into martensite due to the higher nucleation barrier [10]. Finally, there are no dislocations within the fine austenite cells; while dislocations, usually reduces the nucleation barrier for the martensitic transformation. The combination of the above factors make the Ms point reduce to a temperature below the room temperature, so that the martensitic transformation was not triggered.

5. Conclusion

High current pulsed electron beam creates very interesting and intriguing surface modifications such as craters as well as the formation of metastable ultrafine structures. At low number of pulses, the presence of carbides served as nucleation sites for the surface eruption phenomena that creates craters on the surface. At high number of pulses, most of the carbides in the suface layer are dissolved and more homogeneous melted layers are formed on the surface of D2 steel. The microstructure of the melted layers is then composed of ultrafine austenite and nanosized carbides. Even if the cooling rate is very high ($\sim 10^7$ K/s), the martensitic transformation could be completely supperssed. The stabilization of the γ phase must be related to the refinement and alloying (Cr and C) of the autenite grown from the melt.

References

[1] A.D. Pogrebnjak, V.S. Ladysev, N.A. Pogrebnjak, A.D. Michaliov, V.T. Shablya, A.N. Valyaev, A.A. Valyaev, V.B. Loboda, Vacuum 58 (2000) 45–52.
[2] X.Y. Le, S. Yan, W.J. Zhao, B.X. Han, Y.G. Wang, J.M. Xue, Surf. Coat. Technol. 128/129 (2000) 381–386.
[3] A.B. Markov, V.P. Rotshtein, Nucl. Instr. Meth. Phys. Res. B 132 (1997) 79–86.
[4] D.I. Proskurovsky, V. Rotshtein, G.E. Ozur, A.B. Markov, D.S. Nazarov, J. Vac. Sci. Tech. A 1694 (1998) 2480–2488.
[5] C. Dong, A. Wu, S. Hao, J. Zou, Z. Liu, P. Zhong, A. Zhang, T. Xu, J. Chen, J. Xu, Q. Liu, Z. Zhou, Surf. Coat. Technol. 163/164 (2003) 620–624.
[6] Y. Qin, C. Dong, X.G. Wang, S.Z. Hao, A.M. Wu, J.X. Zou, Y. Liu, J. Vac. Sci. Tech. A 21 (2003) 1934–1938.
[7] J.X. Zou, Y. Qin, C. Dong, S.Z. Hao, A.M. Wu, X.G. Wang, J. Vac. Sci. Tech. A 22 (2004) 545–552.
[8] T.Y. Hsu, Martensitic Transformation and Martensite, Science Press, Beijing, 1999.
[9] G.N. Haidemenopoulos, M. Grujicic, G.B. Olson, M. Cohen, J. Alloys Compd. 220 (1995) 142–147.
[10] Q.P. Meng, Y.H. Rong, T.Y. Hsu, Phys. Rev. B 65 (2002) 174118.